

INVESTIGATING THE EFFECTS OF GEL CASTING PARAMETERS ON THE SUSPENSION RHEOLOGY AND MECHANICAL PROPERTIES OF TITANIUM CARBIDE GREEN BODY

In this paper the chemo-rheological behavior of aqueous TiC suspension and physical properties of gelcasted green body were investigated. The monomer system used in this project was acrylamide (AM) and methylenebisacrylamide (MBAM). Polymerisation reaction was promoted by the addition of tetramethyl ethylenediamine as a catalyst and ammonium persulfate as a initiator. The effects of tetramethylammonium hydroxide (TMAH), polyethylenimine (PEI) and polyethylene glycol (PEG) dispersants on the premix solution containing TiC powder have been studied via observation of the zeta potential and rheological behavior. The optimal amount of TMAH was achieved 0.4 wt.% at pH 9. The chemorheological results showed that the gelation time decreased and viscosity increased with increasing the monomer content, solid loading, initiator amount and temperature. The highest flexural strength of gel casted green body was obtained with 50 vol% solid loading and 25 wt.% monomers content.

Keywords: Titanium Carbide, Gel-casting, Rheological Behavior, Gelation time, Viscosity

1. Introduction

Because of good mechanical properties, corrosion resistance, excellent wear resistance and good thermal properties such as low coefficient of thermal expansion and high thermal conductivity of TiC, it was introduced as a superior candidate for improving mechanical properties and has been widely used for high temperature applications [1-5]. However, it is difficult to produce ceramic bodies with complex shapes and accurate dimensions by the conventional forming techniques. For many of these applications, the gelcasting process is extensively used [6-9].

Gel casting is a novel forming technique for fabricating ceramic green parts with near-net shapes, possibility of complex shaping, cost effectiveness, simplicity, high quality final products and flawless structure. It is a promising technology combining advantages has been widely used for producing high-integrity ceramic components [10]. In gelcasting, a concentrated ceramic slurry is created by mixing a ceramic powder and a monomer solution. During the process of these suspension-based forming techniques and in order to produce ceramic products with good performance, dimensional stability and high green strength, it is important to yield suitable suspensions with as high solids loading and low viscosity as possible [11,12].

The rheology of suspension and the physical properties of the ceramic green body are quite dependent on many factors. For example, they are easily affected by dispersant type, monomer

composition, monomer content, monomers ratio, amounts of initiator and catalyst additives, solid loading and temperature [13-15]. So far, a lot of studies have been conducted to investigate the effects of various dispersants on rheological behavior of different aqueous ceramic suspensions such as Al₂O₃, SiC, YSZ, TiC and Si₃N₄ suspensions [16-21]. But up to now, a few studies have been conducted on the chemorheological aspects of gelcasting systems and on the influences of the gelcasting parameters on the properties of the green body. A number of researchers investigated chemorheology of aqueous-based ceramic suspensions during gelation process but the idle time, as a very important factor in processing, was undeterminable [22,23].

In this paper, the chemorheology of gelation of aqueous based TiC suspensions was investigated using viscometry technique. The effect of various parameters such as monomer content, monomer ratio, initiator and catalyst amounts, solid loading and temperature on the idle time, viscosity and mechanical properties were considered and discussed.

2. Experimental

Aqueous gelcasting of TiC was carried out using acrylamide (C₂H₃CONH₂, AM) as a monomer, N,N'-methylenebisacrylamide [(C₂H₃CONH)₂CH₂, MBAM] as a cross-linker, N,N,N',N'-tetramethylethylenediamine (TEMED) as a catalyst and ammonium persulphate as an initiator. The commercial high-

* NUCLEAR FUEL CYCLE RESEARCH SCHOOL, NUCLEAR SCIENCE AND TECHNOLOGY RESEARCH INSTITUTE, TEHRAN, IRAN

** DEPARTMENT OF MATERIALS SCIENCE AND ENGINEERING, MUT, TEHRAN, IRAN

Corresponding author: hforatirad@aeoi.org.ir

purity titanium carbide with an average particle size of 3–5 μm was used as the raw material. Tetramethylammonium hydroxide (TMAH), Polyethylene imine (PEI) and Polyethylene glycol 400 were used as the dispersants. The quantity of dispersants applied with respect to the previous studies [25], were selected at the 0.4, 2 and 0.5 wt% of the ceramic powder, respectively. In the gelcasting process, first the TiC ceramic powder was added to a premix solution containing dispersant and organic monomers. The slurry was degassed for 10 min when the initiator and catalyst were added. The slurries were degassed for another 10 min after casting in the mold. After the monomers had polymerized, the green bodies were demolded. After gelcasting, the samples were dried in a commercial oven, at 60°C with relative humidity of 70% for 60 h.

At first, the influence of various dispersants and solids loading on the zeta potential and rheological behavior of TiC suspension was investigated. And then, various monomer premix solutions, with different monomer contents, monomers ratio and initiator contents were prepared and the gelation behavior of these systems in the presence or absence of ceramic powder and at different temperatures was investigated and compared with each other. Gelation was initiated immediately after adding predetermined amounts of initiator and accelerator.

Z-potential measurements were performed by an acoustic and electroacoustic spectrometer (DT-1200, Dispersion Technology Inc., Bedford Hills, NY). The zeta potentials were recorded as a function of the pH of the suspension. The titration was automatically performed by means of a built-in autotitrator using 0.1M HCl and 1M NaOH solutions. The shear viscosity and the time dependency of pre-mix solutions and viscosities during gelation were measured by a Visco 88 viscometer with a concentric-cylinder having a diameter of 30 mm. Steady state shear flow curves were measured in a shear rate range between 0.03 and 200 S^{-1} . A digital thermometer (i.e. pH-mV-temperature meter with an accuracy of 0.1°C, Lutron TM-905, Taiwan), was used to measure the temperature of pre-mix solutions and suspensions during the progress of gelation. The bending strength of the dried samples were determined by a three-point flexure test in accordance with ASTM C1161 with Universal Testing Machine (ZWICK, Z050) at 0.5 mm/min loading rate. The fracture surfaces morphologies of the fabricated porous ceramics were investigated by scanning electron microscopy (SEM V18 ZISS).

3. Result and discussion

Zeta potential of TiC powders in the absence of any dispersant in deionized water is shown in Fig. 1. The isoelectric point (IEP) of TiC powders is at pH 3.1. The TiO_2 surface oxide in the presence of water, hydrolyzed to Ti-OH groups. When the pH is lower than the IEP, Ti-OH reacts with H^+ leaving Ti-OH_2^+ with positive zeta potentials. When the pH is higher than the IEP, Ti-OH reacts with OH^- , yielding Ti-O^- with negative zeta potentials [26]. Zeta potential of TiC powders in the presence of the monomer (premix solution), was decreased compared to

TiC suspension without dispersant. It suggests that the uncharged monomer molecules screen the charge developed at the solid/liquid interface and decrease the stability of suspension [27]. TMAH dispersant dissociates to $(\text{CH}_3)_4\text{N}^+$ and OH^- in the presence of water [26] and Hydroxyl group promotes the production Ti-O^- inducing more negative charge on the TiC surface. The IEP of TiC suspension disappeared with 2 wt. % PEI addition (Fig. 1) and a highly positive surface charge was achieved at the low pH. PEI is a cationic polymer with repeating unit composed of the amine group and two carbon aliphatic CH_2CH_2 spacers. When an amino group is protonated, it will be attracted to the negatively charged Ti-O^- surfaces group. The protonation of the amine groups in PEI molecules and subsequent expansion of the polyions due to the mutual charge repulsion are responsible for highly positive zeta potential in the wide pH range (positive zeta potential with a value of 30 to 44 mV was obtained in the pH range 5 to 10). In the high pH range (pH > 10), PEI actually carries no charge and the polymers exist as free molecules and thus zeta potential values decrease gradually. PEG is a nonionic dispersant and in the presence of the PEG, the surface charges remain unaffected. In low concentrations, long chain molecules of PEG are absorbed on the surface of TiC particles and by increasing the thickness of the electric double layer, zeta potential slightly increases. The results show that the TMAH dispersant provides good dispersion compared with the PEI and PEG dispersant [29].

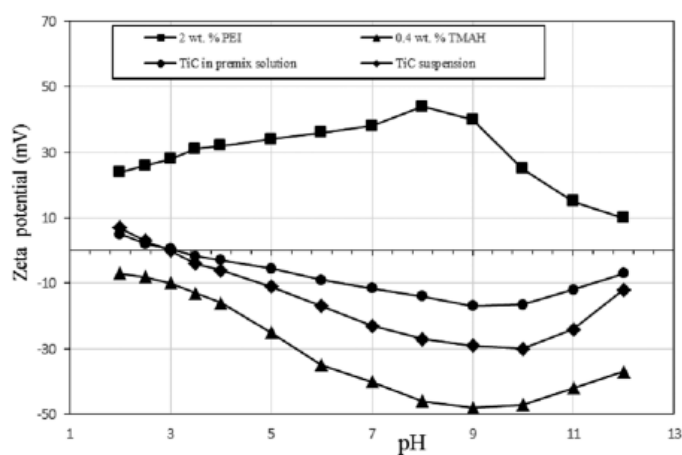


Fig. 1. Zeta potential of TiC suspension without dispersant and TiC in the premix solution with and without dispersant

Fig. 2 shows the effect of dispersant concentrations on the viscosity of premix solutions containing 50 vol. % TiC, 20 wt. % monomers content (AM + MBAM) and the ratio AM/MBAM of 10, as a function of shear rate at the pH = 9. In any concentration, the flow curve deviates from a Newtonian behavior or shear thinning behavior. This behavior is characterized by the decrease in viscosity at increasing shear rates [30]. It is obvious that the viscosity of the slurry decreases with an increase in the dispersant dosage. It is worth mentioning that an optimum concentration of the dispersant is 0.4 wt. %. The viscosity of slurries increases gradually as the concentration of the dispersant increases to 0.6 wt. %. Additional dispersant ions cause the com-

pressive effect on the electrical double layer (EDL) and so, the thickness of the charge cloud on the surface of titanium carbide particles decreases, thereby decreasing the repulsive forces and suspension stability.

Fig. 3 shows the rheological properties of the TiC suspensions vs. different solids loading at the 0.4 wt. % dispersant. It can be seen from the curves that the suspensions in all of the solid loading show shear thinning behavior and belong to pseudoplastic fluid. It also can be found from the curves that the viscosity of suspension increases with the solid loading again. In the solid loading below the 50 vol. %, suspension viscosities are lower than 1 Pa.s and to be enough to provide the required stability to the slurry. There is a substantial increase in the viscosity, when solid loading reaches 60 vol. %. The viscosity increases to >1 Pa.s at shear rate of 75 s^{-1} , which is not suitable for the gelcasting process [30].

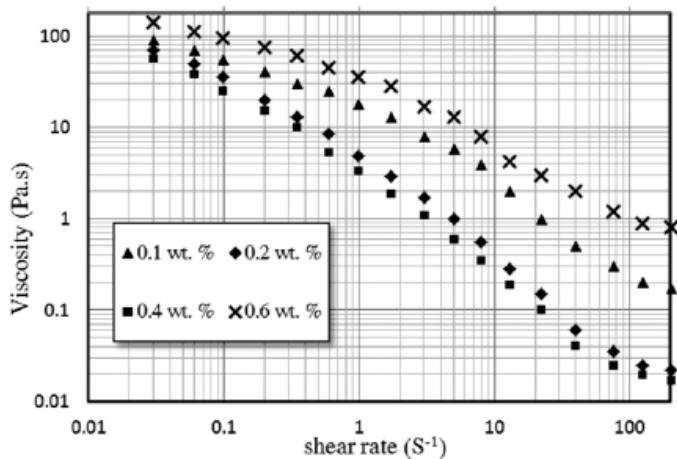


Fig. 2. The effect of dispersant concentrations on the viscosity of premix solutions containing 50 vol. % TiC

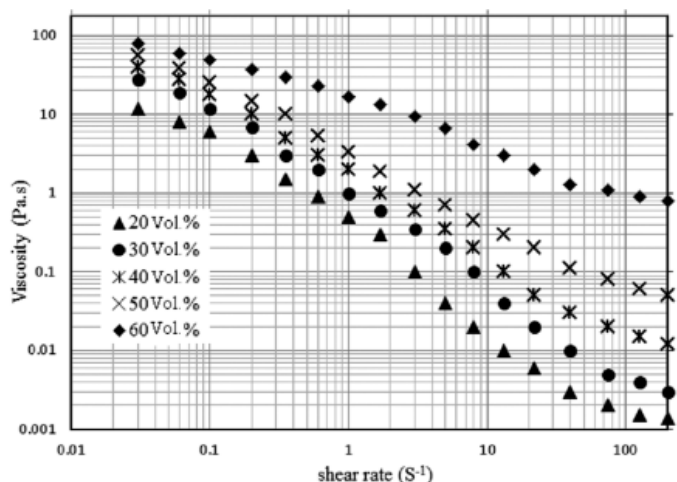


Fig. 3. Variation of viscosity with the solid loading in the 0.4 wt. % TMAH dispersant at different shear rates

Fig. 4 shows the fracture surface of the resulted green body (20 wt. % monomers content, 50 vol. % solid loading and 0.4 wt. % dispersant) with a compact and homogeneous distribu-

tion appearance and a limited number of pores. As seen in the figure, the TiC powders have been almost uniformly dispersed and also the grains are connected by 3D polymeric networks which are responsible for the strength of the green body. The limited number of the holes in the sample can also be caused by the air caption in the gelcasting process.

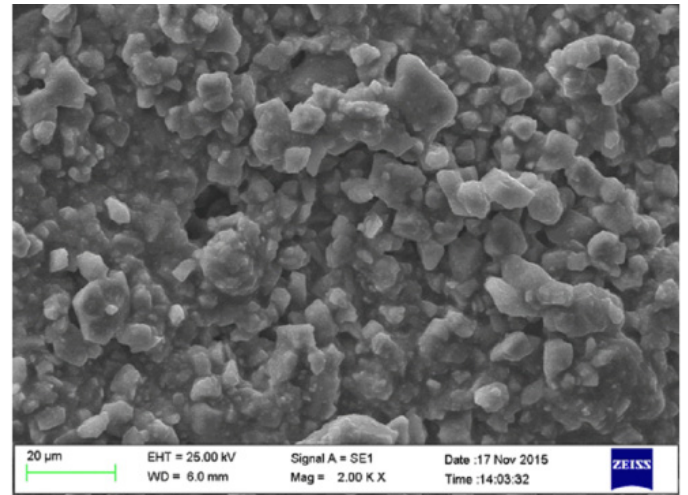


Fig. 4. SEM micrograph of fracture surface of TiC green body gelcasted with 0.4 wt. % dispersant

The radical polymerization of acrylamide is an exothermic reaction. The heat of acrylamide polymerization (19.8 ± 0.7 Kcal/mol) [31], becomes a heat source increasing the system temperature. Thus, the initiation of polymerization in pre-mix can be determined by changes in the temperature of solution. The idle time, t_{idle} , i.e. the time between the addition of the initiator and the catalyst and the beginning of polymerization that is equivalent to the time available for casting the slurry, can be monitored. Idle time is affected by several factors such as monomer concentration, monomer to cross-linker ratio, initiator concentration, amount of solid loading and solution temperature.

Figure 5, shows the changes in the t_{idle} and solution viscosity of a pre-mix solution as the function of monomer content and gelation time, respectively, with constant monomer ratios, initiator and accelerator at 23°C . As shown in Fig. 5a, idle time decreases with the increase of monomer concentration and as seen in Fig. 5b, viscosity increases relatively slow during a certain period and then increases rapidly with increasing monomer content. The higher the concentration of the monomer, the faster polymerization. It is due to an increase in the polymer chain length and formation of intermolecular crosslinking through more crosslinking sites at intence concentrations of the polymer. Hence, the gel formation reaction increases, which decreases the gelation time. In the low monomer content, the polymer chains are too distant from each other and to form intermolecular crosslinking readily [32].

Fig. 6 shows the gelation time and viscosity changes versus various concentrations of AM with constant other parameters. According to the diagram, the gelation time reduced and the viscosity increased with an increase in AM concentration as

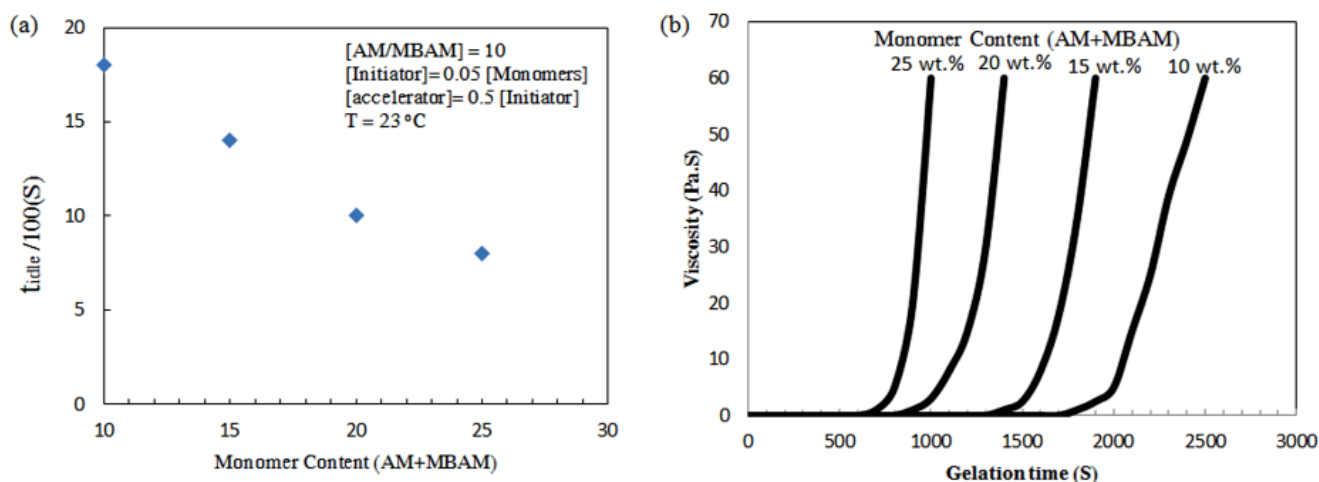


Fig. 5. (a) t_{idle} as a function of the monomer contents and (b) apparent viscosity as a function of the gelation time

a germ of polymerization. The gelation of a polymer with high molecular weights will be faster than the polymers with lower molecular weights. The higher the amount of AM, the increased the polymer chain length and the average molecular weight of polymer chain. As the molecular weight increases, the probability for a polymer chain to form entanglements with the neighboring polymer chains increases and therefore the probability of polymerization reaction increases [33,34].

The role of MBAM concentration on gelation kinetic of solution and viscosity of pre-mix solution with constant AM and APS concentrations in 23°C can be found from Fig. 7. The results showed that the gelation time decreases and the viscosity increases with increasing MBAM concentration as a cross-linker. Polymer chains are often interconnected to form a nonlinear, branched, or crosslinked polymer. Branching is analogous to the extra arms growing out of a polymer chain; thus, the probability of the entangled, physical connections among the chains increases with the MBAM concentration increase. Comparing Figs. 6 and 7 shows that AM concentration affects the idle time and viscosity more significantly than MBAM concentration (higher slope) [35].

Fig. 8 shows the variation of the gelation time and viscosity of pre-mix solutions with respect to the amount of the initiator (APS) with constant AM and MBAM concentration at 23°C. As seen in the figure, the reduction of the initiator concentration increases t_{idle} and decreases the viscosity. Polymerization is initiated by the generation of free radicals from persulfate, so that an increase in APS amount results in a decrease in t_{idle} . Dependence of gelation time and viscosity on the solid loading is shown in Fig. 9. AM and MBAM molecules can be absorbed by TiC particles, increasing the concentrations of the monomers and cross-linkers around the particles increases. As a result, it becomes easier for the MAM and MBAM in the slurry to copolymerize and so the idle time is reduced significantly. The variation of the gelation time and viscosity with pre-mix solution temperature is shown in Fig. 10. The results show clearly that the gelation time is decreased when the temperature of pre-mix solutions is increased. Temperature has a direct effect on the rate of gel polymerization; the polymerization reaction is also exothermic. Consequently, the generated heat quickens the reaction, considerably. Thus, gelation usually occurs very rapidly once polymerization begins.

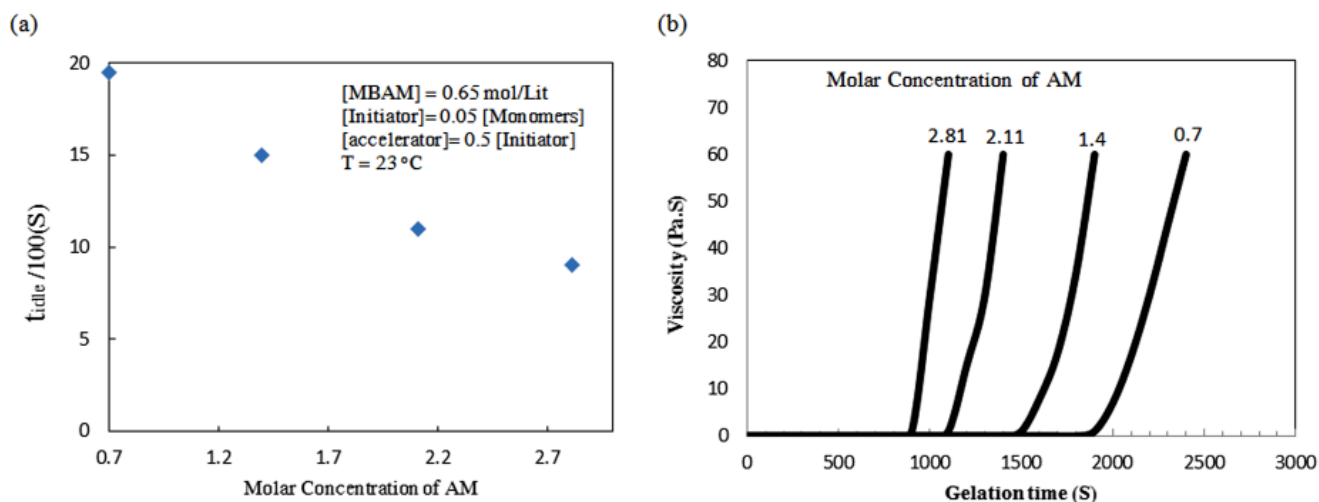


Fig. 6. (a) t_{idle} as a function of the AM concentration and (b) apparent viscosity as a function of the gelation time

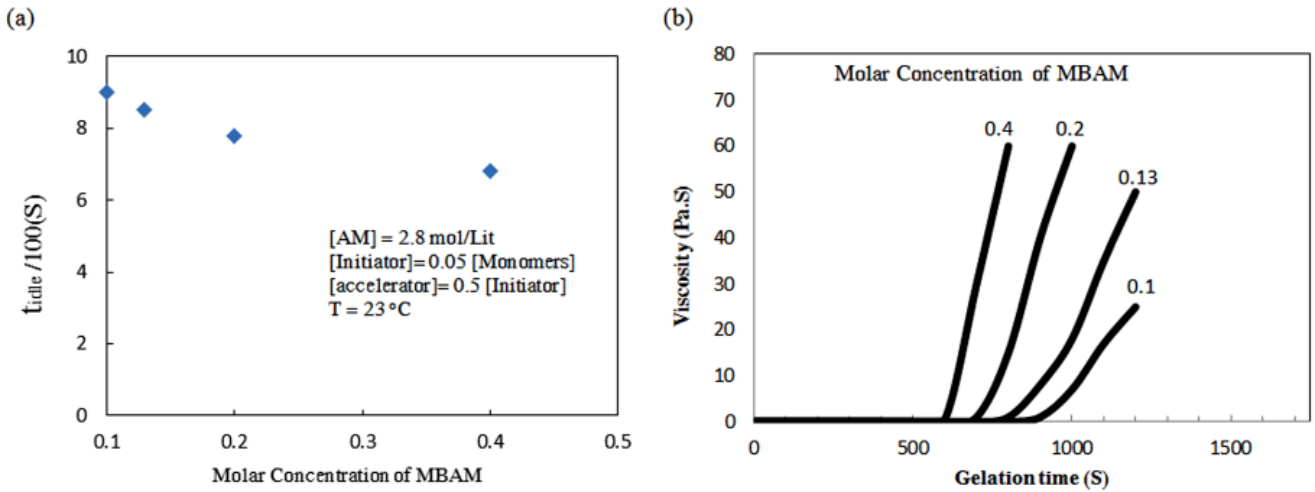


Fig. 7. (a) t_{idle} as a function of the MBAM concentration and (b) apparent viscosity as a function of the gelation time

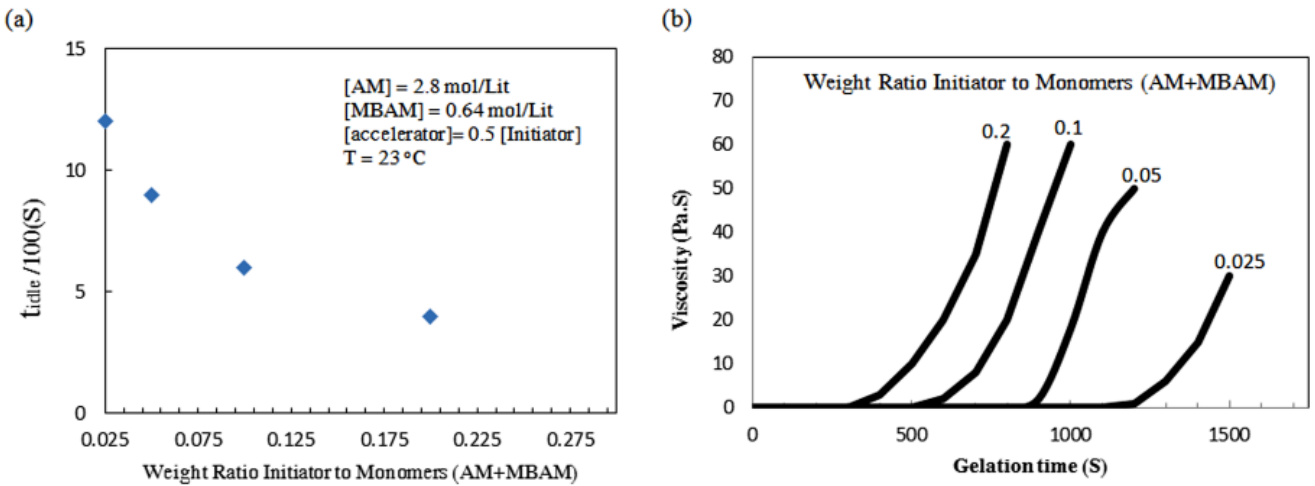


Fig. 8. (a) t_{idle} as a function of the initiator to monomers ratio and (b) apparent viscosity as a function of the gelation time

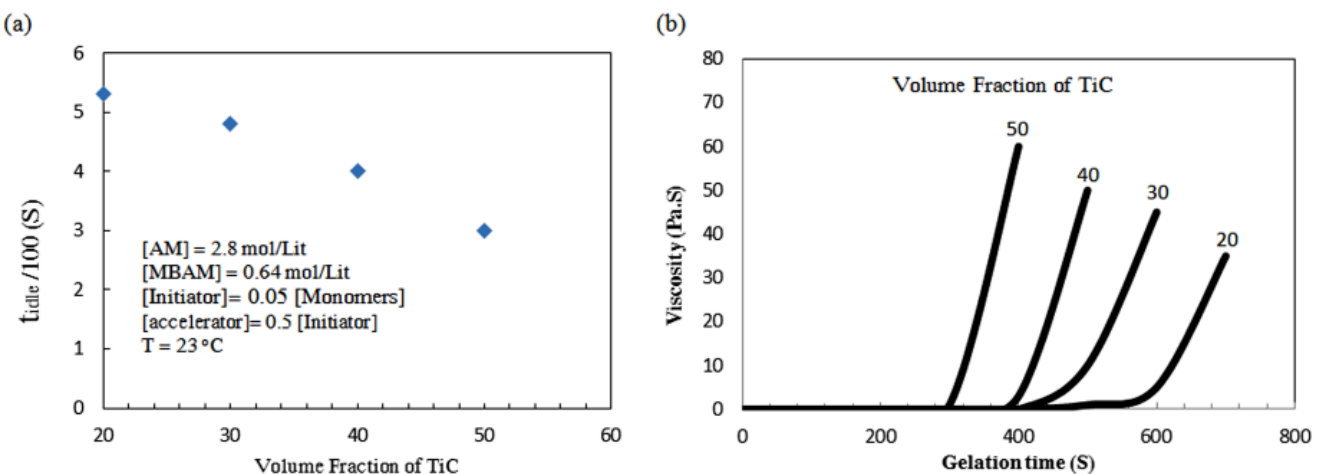


Fig. 9. (a) t_{idle} as a function of the ceramic loading and (b) apparent viscosity as a function of the gelation time

The relationship between the gelation time and the temperature may be expressed by the Arrhenius equation: $t_{idle} = A \exp \frac{E_a}{RT}$ [36]. Where, t_{idle} is the gelation time, A is the pre-exponential factor, R is the universal Gas Law constant, T is the temperature

in kelvin and E_a is the activation energy for the gelation reaction. Fig. 11 illustrates the semi log plots of t_{idle} as a function of inverse of temperature (T^{-1}), for both pre-mix solution and the slurry with 50 vol.% of TiC powder. A plot of $\ln t_{idle}$ vs $1/T$ will yield a slope equal to E_a/R which is used to calculate the

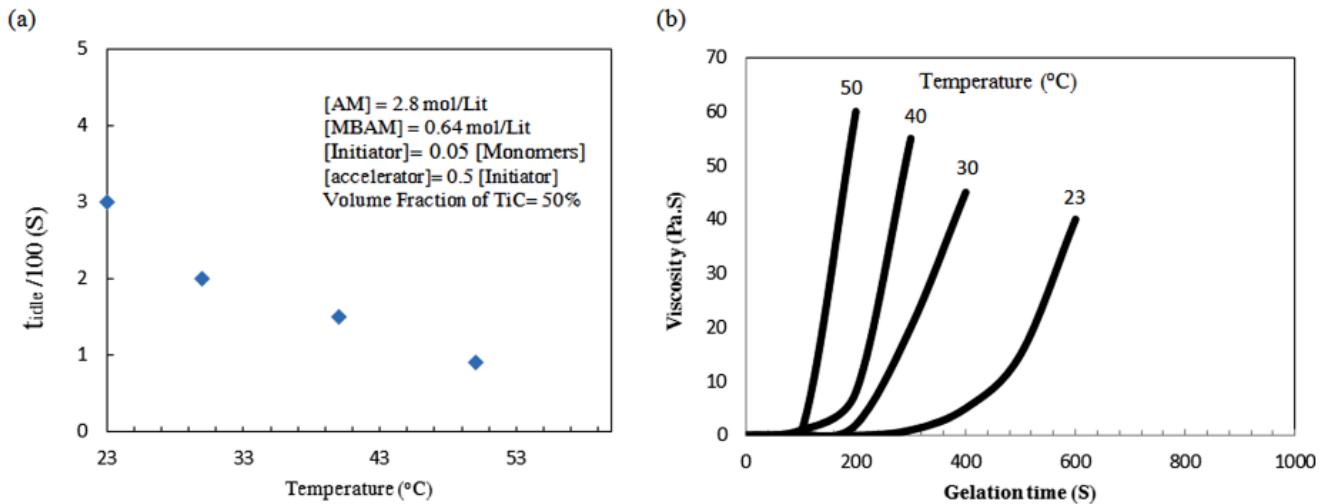


Fig. 10. (a) t_{idle} as a function of the temperature and (b) apparent viscosity as a function of the gelation time

activation energy of the gelation reaction. The activation energy was found to be 55.54 and 39.61 kJ/mol for 0 and 50 vol.% solid loading, respectively. The calculated values of activation energy detect the catalytic effect of ceramic powder on the gelation kinetics of suspensions. Babaluo et al. [37] reported 98.7 and 50.4 kJ/mol values for the activation energy of alumina-aqueous acrylamide gelcasting system with 0 and 35 Vol.% solid loading, respectively. The smaller amounts of activation energy of gelation in this paper could be due to the higher amount of monomer and solid loading.

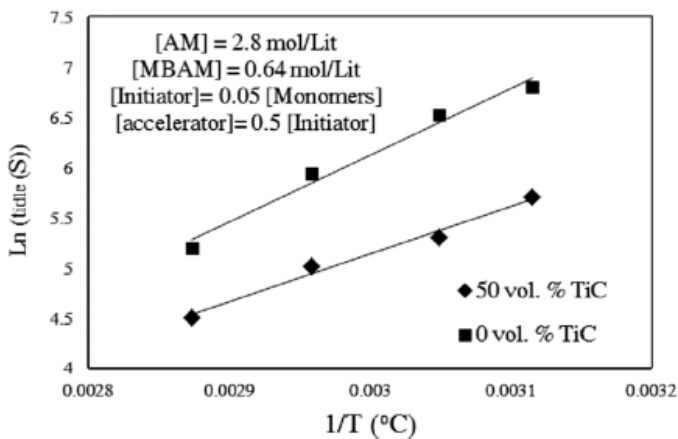


Fig. 11. Arrhenius plot of the gelation time versus inverse gelation temperature

The variation of bend strength of the green bodies as a function of monomers ratio and monomer content for 40 vol.% solid loading is presented in Fig. 12. As seen in the figure, in different monomer contents, the flexural strength of green bodies shows similar trends with the monomers ratio change. At first, the flexural strength increases with the monomers ratio increase until it reaches a maximum value at 12.5 ratios, then decreases for higher monomers ratio. Crosslinking forms bridges between the chains and dramatically increases molecular weight. Consequently, the physical and mechanical properties vary with the composition

and extent of the crosslinking for a given polymer system. The three-dimensional network of crosslinked polymers increases the rigidity. When the monomers ratio is low, the cross-linker is excessive and the three dimensional network structures of the cross-linked polymer are coarse so as to decrease the toughness of network structures and then the flexural strength of the green body decreases [38]. On the other side, when the monomers ratio is too high, the three dimensional network structures are loose, thereby reducing the flexural strength of green body [34].

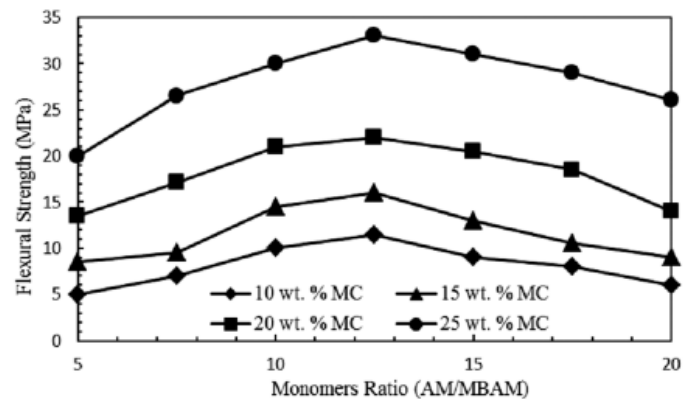


Fig. 12. Dependence of the strength of green gelcast TiC on the monomer content as a function of monomer ratio for the 40 vol.% solid loading

Fig. 13 shows the influences of monomer content and solid loading on the bending strength of the green body. The bending strength of TiC green body in the 25 wt.% monomer content with 50% solid loading was the highest, reaching about 39 MPa, while the bending strength with 20, 30 and 40% solid loading were about 21, 29 and 33 MPa, respectively. The higher amount of the monomer content results in the increased polymer chain length and the bridging sites. The longer the polymer chain, the greater the numbers of entanglements that can form along it. Therefore, the longer the chain, the more difficult it is to distort the polymeric material. In addition to the linear macromolecules,

polymer chains are often interconnected to form a nonlinear, branched, or crosslinked polymer. In the maximum value of the monomers content and solid loading, the three-dimensional network of the cross-linked polymer gels is compact and the cross-linked gel network adheres to the TiC particles and binds them together, providing the way for a uniform distribution of TiC powders in the green body. The results suggest that the bending strength increase with increasing the monomer content and solid loading [39].

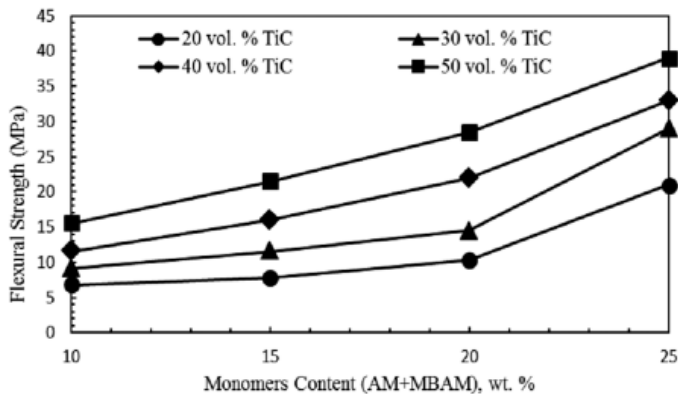


Fig. 13. The bending stress of green gelcast TiC with varied solid loading as a function of monomer content

Fig. 14 shows the influences of monomer content and solid loading on the shrinkage rate of the green body. Increasing the monomer content and solid loading decreases the shrinkage rate of TiC green body. The decrease could be attributed to the strengthened 3D macromolecular network (as a result of the higher amount of the monomer content and solid loading), which helps to resist further contraction caused by the water evaporation. However, the higher solid loading means less inter-particle spacing and thus less water would be removed from the gel casted body resulting in smaller shrinkage which would occur during drying [39].

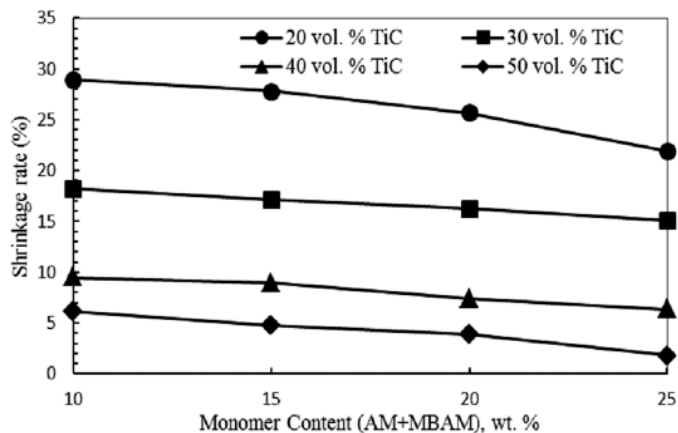


Fig. 14. The influences of monomer content and solid loading on shrinkage rate of TiC green body

4. Conclusion

We have studied the rheological behavior of TiC suspension and the structure evolution of titanium carbide green body.

- The rheological tests results showed that TMAH can significantly improve the dispersibility of TiC powder compared to the other dispersants. In the present of TMAH, the zeta potential of TiC suspension increased to -48 mV at the pH value 9.
- The chemorheological tests results showed that the increase in the monomer content, AM and MBAM concentration, initiator amount and temperature decreased the gelation time. It was found that the ceramic suspensions exhibit virtually an infinitesimal idle time compared to the pure monomer premixes.
- The green strength TiC bodies prepared by gelcasting was shown to vary from ~ 5 MPa to over 39 MPa, depending on the solid loading, amount of monomers, and monomers ratio. The greatest strength was obtained with the gel casted samples containing 50 vol% solid loading, 25 wt.% monomers, and a monomer ratio of 12.5.

Conflict of interest

The authors declare that they have no conflict of interest.

REFERENCES

- [1] R.F. Voitovich, E.A. Pugach, Powder Metal. Met. **11** (2), 132-136 (1972).
- [2] R. Dash, J. Chmiola, G. Yushin, Y. Gogotsi, G. Laudisio, J. Singer, J. Fischer, S. Kucheyev, Carbon **44**, 2489-2497 (2006).
- [3] M.S. Kovalchenko, Refract. Met. Hard. Mat. <http://www.sciencedirect.com/science/journal/02634368> **39**, 32-37 (2013).
- [4] D. Cedat, M. Libert, M. Le flem, O. Fandeur, C. Rey, M. Clavel, J. Schmitt, Refract. Met. Hard. Mat. **27**, 267-273 (2009).
- [5] M. Gherrab, V. Garnier, S. Gavarini, N. Millard-Pinard, S. Cardinal, Refract. Met. Hard. Mat. **41**, 590-596 (2013).
- [6] N. Lin, Y. He, C. Wu, S. Liu, X. Xiao, Y. Jiang, Refract. Met. Hard. Mat. **46**, 52-57 (2014).
- [7] E. Adolfsson, Am Ceram Soc. **89**, 897-1902 (2006).
- [8] Z. Yi, Z. Xie, J. Ma, Y. Huang, Y. Cheng, Mater. Let. **56**, 895-900 (2002).
- [9] A. Najafzadeh, A. Habibolahzadeh, F. Qods, H.R. Baharvandi, Refract. Met. Hard. Mat. **46**, 30-34 (2014).
- [10] O.O. Omatete, M.A. Janney, R.A. Strelow, Am. Ceram. Soc. Bull. **70**, 1641-1649 (1991).
- [11] D. Jiang, J. Ceram. Soc. Jap. **116**, 694-699 (2008).
- [12] D. Jiang, Key. Eng. Mat. **403**, 163-164 (2009).
- [13] X. Wang, R. Wang, C. Peng, H. Li, Mat. Inter. **22** (4), 347-353 (2012).
- [14] D. Liu, J. Mat. Sci. **35** (21), 5503-5507 (2000).
- [15] T. Dabak, O. Yucel, Rheo. Acta. **25** (5), 527-533 (1986).

- [16] D. Liu, *J. Mat. Sci.* **35** (21), 5503-5507 (2000).
- [17] J.A. Yanez, T. Shikata, F.F. Lange, D.S. Pearson, *Am. Ceram. Soc.* **79** (11), 2917-2924 (1996).
- [18] W. Li, P. Chen, M. Gu, Y. Jin, *Euro. Ceram. Soc.* **24** (14), 3679-3684 (2004).
- [19] X. Li, C. Zou, T. Wang, X. Lei, *J. Heat Mass Trans.* **84**, 925-930 (2015).
- [20] S. Moghadas, A. Maghsoudipour, M. Alizadeh, T. Ebadzadeh, *Ceram. Inter.* **37** (16), 2015-2019 (2011).
- [21] L. Xuejian, H. Liping, X. Xin, F. Xiren, G. Hongchen, *Ceram. Inter.* **26** (3), 337-340 (2000).
- [22] J.S. Chong, E.B. Christiansen, A.D. Baer, *J. App. Poly. Sci.* **15** (8), 2007-2021 (1971).
- [23] H. Sarraf, J. Havrda, *Ceramics – Silikáty* **51** (3), 147-152 (2007).
- [24] C. Martinez, A. Lewis, *J. Am. Ceram. Soc.* **85** (10), 2409-16 (2002).
- [25] H. Foratirad, H. R. Baharvandi, M. G. Maragheh, *Refract. Met. Hard Mat.* **56**, 96-103 (2016).
- [26] J. Zhang, D. Liang Jiang, S. Hong Tan, L. Gui, and M. Ruan, *Amer. Ceram. Soc.* **84** (11), 2537-2541 (2001).
- [27] Q. Zhang, W. Li, M. Gu, Y. Jin, *Powder Tech.* **161**, 130-134 (2006).
- [28] Q. Huang, P. Chen, M.Y. Gu, Y.P. Jin, K. Sun, *Mater. Lett.* **56**, 546-553 (2002).
- [29] M.D. Vljajic, V.D. Krstic, *J. Mat. Sci.* **37**, 2943-2947 (2002).
- [30] L. Bergstrom, *Physico. Eng. Aspect.* **133**, 151-155 (1998).
- [31] M. Orban, K. Kurin, A. Zhabotinsky, I. Epstein, *J. Phys. Chem. B.* **36**, 36-40 (1999).
- [32] A. Pethrick, A. Ballada, G.E. Zaikov, *Handbook of Polymer Research: Monomers, Oligomers, Polymers and Composites*, 2007 Nova Science Publisher.
- [33] H. Winter, M. Mours, *Rheology of Polymers Near Liquid-Solid Transitions Advances in Polymer Science*, 1997 Springer.
- [34] K. Matyjaszewski, P. Davis, *Handbook of Radical Polymerization*, 2002 John Wiley & Sons. Inc. Publication.
- [35] M. Kriss, *Handbook of Digital Imaging*, 2015 John Wiley & Sons, Inc. Publication.
- [36] U. Yadav, V. Mahto, Investigating the Effect of Several Parameters on the Gelation Behavior of Partially Hydrolyzed Polyacrylamide-Hexamine-Hydroquinone Gels, *Indust. Eng. Chem. Research.* **52** (28), 9532-9537 (2013).
- [37] A. Babaluo, M. Kokabi, A. Barati, *Euro. Ceram.Soc.* **24**, 635-644 (2004).
- [38] H. Wang, S. Jia, Y. L. Wang, Z. H. Jin, *J. Xi'an Jiaotong Univer.* **35**, 403-406 (2001).
- [39] J. Yu, H. Wang, H. Zeng, J. Zhang, *Ceram. Int.* **35**, 1039-1044 (2009).